20. C. D. Charles and R. G. Fairbanks, *Nature* **355**, 416 (1992).
21. Percent of GNAIW = [($\delta^{13}C_{\text{eastern basin water}}$ − $\delta^{13}C_{SOW}$)/($\delta^{13}C_{GNAIW}$ − $\delta^{13}C_{SOW}$) × 100%].
22. W. B. Curry and G. P. Lohmann, *Paleoceanography* 5, 487 (1990).
23. N. C. Slowey, thesis, Massachusetts Institute of Technology–Woods Hole Oceanographic Institution Joint Program (1991); ____ and W. B. Curry, *Nature* **358**, 665 (1992).
24. E. A. Boyle, in *Mesozoic and Cenozoic Oceans*, K. J. Hsü, Ed. (American Geophysical Union, Washington, DC, 1986), pp. 49–60.
25. L. D. Labeyrie *et al., Quat. Sci. Rev.* 11, 401 (1992).
26. L. L. Labeyrie and J. C Duplessy, *Palaeogeogr. Palaeoclimatol. Palaeocol.* **50**, 217 (1985).
27. D. W. Oppo and R. G. Fairbanks, *Paleoceanography* **4**, 333 (1989).
28. G. H. Rau, T. Takahashi, D. J. Des Marais, *Nature* **341**, 516 (1989).
29. P. S. Liss and L. Merlivat, in *The Role of Air-Sea Exchange in Geochemical Cycles*, P. Baut-Menard, Ed. (Reidel, Hingham, MA, 1986), pp. 113–127; W. S. Broecker and E. Maier-Reimer, *Global Biogeochem Cycles* **6**, 315 (1992); W. S. Broecker, in preparation.
30. T Veum, E. Jansen, M. Arnold, I Bayer, J -C. Duplessy, *Nature* **356**, 783 (1992).
31. J C. Duplessy *et al., Oceanol. Acta* **14**, 311 (1991)
32. J Carstens and G. Wefer, in (*17*), p 79.
33. A. McIntyre *et al*, in *Investigations of Late Quaternary Paleo-Oceanography and Paleoclimatology*, R. M. Cline and J. D. Hays, Eds. (Geological Society of America, Boulder, CO, 1976), pp. 43–76; W. F. Ruddiman and A. McIntyre, *Palaeogeogr. Palaeoclimatol. Palaeoecol.* **35**, 145 (1981), L. D. Keigwin and E. A. Boyle, *ibid* **73**, 85 (1989); T. B. Kellogg, *Boreas* **9**, 115 (1980).

34. We thank E. Joynt III, E. Franks, and N. Weicker for preparing samples and performing the analyses as well as W. Curry, C. Ravelo, and two reviewers whose comments helped clarify some ideas presented in this report. Supported by NSF grant OCE91-816259. The Lamont-Doherty Geological Observatory Deep-Sea Sample Repository is supported by NSF grant OCE91-01689 and Office of Naval Research grant N00014-90-J-1060.

4 September 1992, accepted 4 December 1992

Order-Disorder Transition in Polycrystalline C_{60} Films

Kelly Akers, Kejian Fu, Peng Zhang, Martin Moskovits*

High-resolution Raman spectroscopy of polycrystalline films of C_{60} deposited under ultrahigh-vacuum conditions show that the spectrum below 244 ± 3 kelvin consists of a superposition of two components whose relative contributions are temperature-dependent. The spectrum of the more intense of the two components is similar to that obtained for air- or oxygen-exposed samples of C_{60} at room temperature, whereas the spectrum above 244 ± 3 kelvin corresponds to one previously reported for oxygen-free samples of C_{60}. The results may indicate an order-disorder phase transition involving the percolation of a cluster of C_{60} molecules engaged in coherent Raman scattering.

In 1985 Kroto *et al.* (*1*) proposed that carbon can exist in one of several molecular cage forms, of which C_{60} is the most celebrated. Two years ago a facile method for the preparation of C_{60} was discovered (*2*), and a large number of the molecular and materials properties of C_{60} and substances derived from it have been determined and reported (*3*). In particular, the vibrational spectrum of C_{60} has been the subject of a large number of papers in the 2 years since the discovery of the facile route for its preparation (*2*). Both infrared and Raman spectra (*4*) have been reported under a variety of conditions including high pressure (*5*) and low temperature (*6*). Despite such an extensive effort on a system that, owing to its high symmetry and the simplicity of its bonding, is vibrationally rather straightforward, the Raman spectroscopy has proven to be rather subtle.

Two distinct Raman spectra have been attributed to solid C_{60}. The first, reported by Bethune *et al.* (*4*), is an intense spectrum characterized by the appearance of the A_g pentagonal pinch band at 1469 ± 1 cm^{-1}. The same mode is observed at 1457 ± 1 cm^{-1} in the second, weaker spectrum, reported by Duclos *et al.* (*7*). The center frequencies of other bands and their relative intensities also differ in the two spectra. For ease of discussion the two spectra will be referred to as the 1470 and the 1458 spectra, corresponding to the frequencies of the A_g pentagonal pinch bands.

Duclos *et al.* attribute the existence of two types of Raman spectra to the fact that solid C_{60} absorbs atmospheric oxygen. They claim that the 1470 spectrum is the oxygenated form of C_{60} whereas the 1458 spectrum is carried by the oxygen-free variety. Oxygenation here implies an interstitial incorporation of oxygen in the C_{60} crystal rather than chemical reaction with C_{60}, to form, for example, the C_{60} epoxide, as reported by Creegan *et al.* (*8*) or by Diederich *et al.* (*9*) for C_{70}.

More recently Tolbert *et al.* (*6*) reported a shift in the frequency of the pentagonal pinch mode of single-crystal C_{60} with temperature. Although they did not indicate whether the measurements were carried out while heating or cooling the crystal, they reported a sudden increase in frequency at ~240 K, reaching a plateau at approximately ~150 K. Although these researchers were unable to record the entire spectrum, the low-temperature spectrum appears to be the 1470 spectrum and the high-temperature spectrum is the 1458 spectrum. In this report we present entire Raman spectra of C_{60} films deposited under ultrahigh-vacuum (UHV) conditions and cycled in temperature between 55 K and room temperature.

It is known that C_{60} undergoes a first-order phase transition at 249 K from a face-centered-cubic (fcc) structure above, to a primitive cubic structure below, this temperature (*10*). As this transition is approached from below, there is evidence of a "precursor state" (*10*) whose nature has not been clarified. Nuclear magnetic resonance (NMR) measurements (*11*) show a sharp break in the T_1 relaxation rate near 249 K, which has been interpreted as a transition between a high-temperature phase in which the C_{60} molecules can rotate freely and a low-temperature phase in which the molecules jump-rotate between symmetry-equivalent orientations (ratchet motion). However, the molecules continue to rotate well below this temperature (*12*).

Purified C_{60} samples were prepared in the now standard fashion (*2*) (carbon arc generation of soot followed by column chromatography). Samples were loaded into a resistively heated evaporator, outgassed before use, and sublimed onto a polished copper surface that was heatable and coolable (55 to 700 K). The entire assembly was contained in a UHV system with bottom pressures below 1×10^{-10} torr. Raman spectra were collected with a SPEX (Metuchen, New Jersey) scanning double monochromator equipped with photon counting and interfaced to a personal computer. Although spectra were collected more slowly than with a multichannel system, this instrument allowed higher resolution and greater wave number accuracy.

Raman spectra obtained with the sample at 57 K, 298 K, and several intermediate temperatures are shown in Fig. 1. The spectrum obtained at the lowest temperature (spectrum B) is similar to the 1470 spectrum of Bethune *et al.* (*4*). The high-temperature spectrum (Fig. 1, spectrum A), on the other hand, is essentially the 1458 spectrum of Duclos *et al.* (*7*). The Raman cross sections of the major bands in the spectrum (compare, for example, the intensities of the pentagonal pinch modes) are some tenfold more intense in the former than in the latter. The details of the spectra obtained in the vicinity of 225 K (spectrum

---

Department of Chemistry and Ontario Laser and Lightwave Research Centre, University of Toronto, Toronto M5S 1A1, Canada.

*To whom correspondence should be addressed.

E) clearly show the coexistence of two spectra. It appears, therefore, that the frequency of the pentagonal pinch mode does not shift appreciably with temperature, as reported by Tolbert *et al.* (6); rather, at temperatures intermediate between ~150 and ~240 K, the spectrum is a superposition of two spectra which, under conditions of low instrumental resolution, gives the impression of shifting in frequency.

We investigated the temperature dependence of this transformation by setting the spectrometer on the 1470-cm^{-1} line (or, alternatively, the 1458 cm^{-1} line) and following its intensity with temperature. It took approximately 8 hours to complete a cycle. Figure 2 shows that the process is very hysteretic. In the cooling half-cycle, the 1470 spectrum does not appear until the temperature is reduced to approximately 120 K. On warming a previously cooled film, one sees a much more gentle decline of the 1470 spectrum (with a simultaneous increase in the 1458 spectrum). With 350-mW laser illumination it is completely replaced by the 1458 spectrum at approximately 213 K. Because laser heating may affect the local temperature of the film, these measurements were carried out for several values of the incident laser power and the transition temperature was corrected, by extrapolation, to zero laser power. These results were repeatable and reversible.

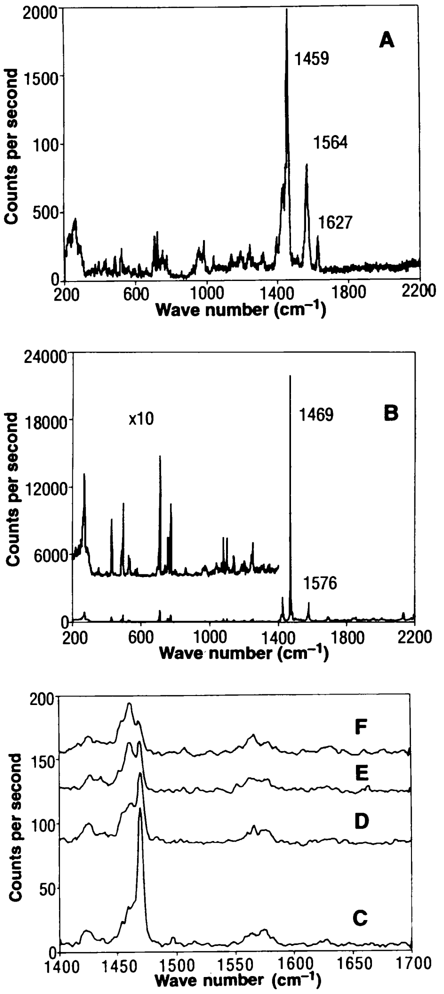

Fig. 1. Raman spectra of C_{60} film recorded under UHV conditions with 488-nm Ar^+ laser excitation at the following temperatures and laser powers: spectrum A, 298 K, 400 mW; spectrum B, 57 K, 400 mW; spectrum C, 212 K, 156 mW; spectrum D, 220 K, 156 mW; spectrum E, 225 K, 156 mW; and spectrum F, 235 K, 156 mW.

Several models were considered to explain these observations. Inspired by the oxygen results of Duclos *et al.* (7), we considered the possibility that an impurity adsorbing from the gas phase was permeating the film. The hysteresis, in this case, would result from the fact that, at low pressures, the isotherm governing the adsorption process allows adequate material to adsorb on the film only at low temperatures. Once saturated, the loss of the impurity upon warming would be governed by diffusion, giving rise to different time evolutions of the Raman intensity in the two halves of the cooling-warming cycle.

Although the appropriate expressions describing these processes fit the data adequately well, the model was invalidated by several experimental observations. First, the low-temperature spectrum was obtained immediately upon depositing the film on a cold surface. Because the film was several hundred angstroms thick, there was not sufficient time to contaminate so large a quantity of C_{60} in so short a time at 1×10^{-10} to 2×10^{-10} torr. Second, the Raman spectrum of a previously cooled film when heated to 150 K did not show any changes; however, the spectrum of a warm film, when cooled to 150 K and then maintained at that temperature, changed to the 1470 spectrum. This result indicated that a previously cooled film remains more or less at equilibrium when it is warmed. Finally, all attempts to change the rates of the processes by dosing with hydrogen and CO, the two most abundant residual gases in the vacuum system, indicated that these two species were not implicated.

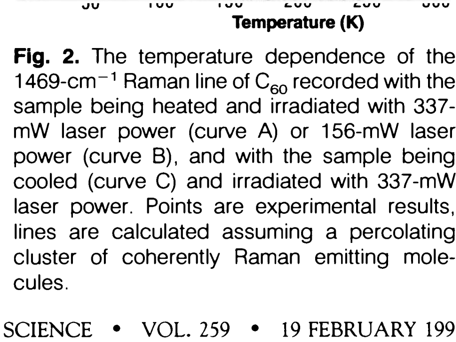

Fig. 2. The temperature dependence of the 1469-cm^{-1} Raman line of C_{60} recorded with the sample being heated and irradiated with 337-mW laser power (curve A) or 156-mW laser power (curve B), and with the sample being cooled (curve C) and irradiated with 337-mW laser power. Points are experimental results, lines are calculated assuming a percolating cluster of coherently Raman emitting molecules.

The temperature dependence of the Raman intensity of the 1470-cm^{-1} line is reminiscent of the behavior of an order parameter in an order-disorder phase transition (*13*). If so, then the observed hysteresis indicates that the disorder can be "frozen in" during the cooling-down half cycle. Taking the intensity of the 1470 cm^{-1} line, $R(T)$, as a measure of an order parameter, Q, defined as $Q = [R(T) - R_\infty]/R_0$, where R_∞ is a base-line correction and R_0 is the low-temperature value of $R(T)$, we found that Q varied with temperature as $(1 - T/T_c)^\beta$ near the critical temperature, T_c, with β values varying between 0.95 and 1.0 and $T_c = 244 \pm 3$ K for three C_{60} films of varying thickness (corrected for laser heating).

Critical exponent values that describe the behavior of an order parameter near the critical temperature depend on the nature of the process (*13*). A value of unity for β is unusual. Only percolation processes in high dimensions are characterized by this value of β. For processes in three or fewer dimensions, critical exponents normally range (*13*) from 0.125 to 0.45. It is unlikely, therefore, that Q is a simple order parameter.

The critical change in the Raman spectrum lies near the first-order phase transition temperature of 249 K. However, the Raman data clearly indicate the coexistence of two phases over a wide range of temperatures, contrary to the nature of first-order transitions. The proximity of the two critical temperatures indicates, however, that there is some relation between the structural changes brought about by the first-order transition and the order-disorder transition implied by the Raman results. Perhaps the so-called precursor state reported by Heiney *et al.* (*10*) is also related to our observation. Moreover, the close similarity of our 1470 spectrum with that observed by Duclos *et al.* (*7*) for oxygen-exposed C_{60} implies that this phase transition can also be induced by impurities such as oxygen dissolved interstitially in the C_{60} crystal.

An order-disorder process consistent with the large increase in Raman cross section on going from the high- to the low-temperature phase is one in which clusters of C_{60} molecules that jump-rotate and vibrate coherently within a matrix of incoherently rotating and vibrating molecules begin to nucleate at 249 K (a visual picture of coherent rotation would be meshing gears). (Alternatively, the low-temperature phase might correspond to molecules that are stationary for much longer than the dephasing time of a normal mode of the cluster.) At T_c (244 ± 3 K) these coherently vibrating molecules percolate, forming the first percolating cluster (referred to as the "infinite cluster" in percolation literature), which grows in size with decreasing temperature, eventually encompassing the entire solid. We propose that the 1470 spectrum corresponds to vibrations of the percolating cluster whose constituent molecules vibrate coherently. Because the vibrational time scale is much shorter than rotational time constants, it is the vibrational coherence that is of primary concern here. Nevertheless, the vibrational coupling may result from the ensured molecular alignment that coherent rotation imposes.

According to this model, the dramatic increase in the Raman cross section on going from the high- to the low-temperature forms of solid C_{60} arises from the cooperative Raman scattering by the constituent particles of the percolating cluster (*14*). In its simplest form, cooperative scattering would be characterized by a total Raman cross section that increases as the square of the number of molecules in the cluster. As the cluster grows large, however, the Raman intensity should increase less rapidly with cluster size (*15*). If the percolating cluster is large enough, one would expect saturation to have been reached at T_c, beyond which the Raman intensity increases proportionally with cluster size. The average cross section per molecule, however, will be larger than that of an equivalent number of independent scatterers. On the basis of our observations, the average size of the percolating cluster at T_c would be at least ten molecules.

Because no great change in the heat capacity is observed below 249 K (*10*), one must assume that the order-disorder transition is geometric rather than thermodynamic. It is also likely that the incorporation of oxygen decreases the volume per C_{60} molecule in a manner similar to thermal contraction, thereby restricting molecular rotation.

One can make these arguments more quantitative. Frisch *et al.* (*16*) reported the results of Monte Carlo calculations to determine the percolation probability, $P(p)$, as a function of the lattice occupation fraction, p. We define $C(p)$ as the fraction of the lattice that belongs to the percolating cluster, that is, $C(p) = pP(p)$. The intensity of the 1470-cm^{-1} line should be proportional to $C(p)$. Using the Monte Carlo data of Frisch *et al.* (*16*) for an fcc lattice, we determined that the value of p at the percolation threshold is $p_c = 0.113$ and that $C(p)$ is well described by the function

$$C(p) = A(p - p_c)^{\theta} \qquad (1)$$

with $A = 1.03$ and $\theta = 0.7$ for $p > p_c$ and $C(p) = 0$ for $p < p_c$. Although the relation between p and temperature is unknown, we assume that coherently vibrating molecules correspond to the lower energy state of a two-state system. Hence p is assumed to take the form

$$p(T) = [1 + b\exp(\Delta H/kT)]^{-1} \qquad (2)$$

The temperature dependence of the intensity of the 1470-cm^{-1} Raman line, expressed as $Q(T)$, was fit to the above expressions for $C(p)$ and $p(T)$, allowing three parameters to vary: ΔH, b, and a scaling constant. A good fit (solid curve in Fig. 2) was obtained over a range of temperatures from approximately 150 K to T_c for the Raman data collected from the three samples studied, with $\Delta H = -4 \pm 1$ kcal mol^{-1} and a value of b consistent with $T_c = 244$ K (when corrected for laser heating). Although $C(T)$ is expected to be nonanalytic at T_c, the experimental results show a slight curvature at T_c that varies with sample thickness, suggesting a finite size effect (*16*). A good fit is not expected for temperatures well below T_c because neither the form of $C(T)$ nor the dependence of the Raman intensity on cluster size are known when the cluster is very large. Nevertheless, the sudden change in slope observed at approximately 100 K (Fig. 2) is reproducible and may signal yet another structural change. The value of ΔH obtained in the fit is reminiscent of the activation energy of the reorientational correlation time for the "ratchet" phase as determined by NMR (*11*).

REFERENCES

1. H. W. Kroto, J. R. Heath, S. C. O'Brien, R. F. Curl, R. E. Smalley, *Nature* **318**, 162 (1985).
2. W. Kratchmer, K. Fostiropoulos, D. R. Huffman, *Chem Phys. Lett* **170**, 167 (1990), W. Kratchmer, L. D. Lamb, K. Fostiropoulos, D. R. Huffman, *Nature* **347**, 354 (1990).
3. *Acc. Chem. Res.* **25** (no. 3) (1992); special issue on Buckmin-sterfullerenes.
4. D. S. Bethune *et al.*, *Chem. Phys. Lett.* **179**, 181 (1991); D. S. Bethune, G. Meijer, W. C. Tang, H. J. Rosen, *ibid.* **174**, 219 (1990).
5. D. D. Klug, J. A. Howard, D. A. Wilkinson, *ibid.* **188**, 168 (1992).
6. S. H. Tolbert, A. P. Alivisatos, H. E. Lorenzana, M. B. Kruger, R. Jeanloz, *ibid.*, p. 163.
7. S. J. Duclos, R. C. Haddon, S. H. Glarum, A. F. Hebard, K. B. Lyons, *Solid State Commun.*, in press.
8. K. M. Creegan *et al.*, *J. Am. Chem. Soc.* **114**, 1103 (1992).
9. F. Diederich *et al.*, *Science* **252**, 548 (1991).
10. P. A. Heiney *et al.*, *Phys. Rev. Lett.* **66**, 2911 (1991).
11. R. Tycko *et al.*, *ibid.* **67**, 1886 (1991).
12. C. S. Yannoni, R. D. Johnson, G. Meijer, D. S. Bethune, J. R. Salem, *J. Phys. Chem.* **95**, 9 (1991); R. Tycko *et al.*, *ibid.*, p. 518.
13. H. E. Stanley, *Introduction to Phase Transitions and Critical Phenomena* (Clarendon, Oxford, 1971).
14. R. H. Dicke, *Phys. Rev.* **93**, 99 (1954); J. C. MacGillivray and M. S. Feld, *Phys. Rev. A* **14**, 1169 (1976); S. G. Rautian and B. M. Chernobrod, *Sov. Phys. JETP* **45**, 705 (1977).
15. J. Grad, G. Hernandez, S. Mukamel, *Phys. Rev. A* **37**, 3835 (1988).
16. H. L. Frisch, J. M. Hammersley, J. A. Welsh, *Phys. Rev.* **126**, 949 (1962).

9 June 1992; accepted 15 December 1992

The Nonhelical Structure of Antifreeze Protein Type III

Frank D. Sönnichsen, Brian D. Sykes,* Heman Chao,
Peter L. Davies

Antifreeze proteins (AFPs) are present in the blood of some marine fishes and inhibit the growth of ice crystals at subzero temperatures by adsorption to the ice lattice. The solution structure of a Type III AFP was determined by two-dimensional nuclear magnetic resonance spectroscopy. These measurements indicate that this 66-residue protein has an unusual fold in which eight β strands form two sheets of three antiparallel strands and one sheet of two antiparallel strands, and the triple-stranded sheets are packed orthogonally into a β sandwich. This structure is completely different from the amphipathic, helical structure observed for Type I AFPs.

The interaction of proteins with solvent water has received much attention, especially the influence of solvent on the stability and folding of proteins (*1*). Less is known about how proteins influence the structure of water. One aspect of this problem is the nature of the interaction near the freezing point of water or at subzero temperatures. Fish AFPs depress the freezing point of water in a noncolligative manner by binding directly to ice crystal nuclei at the interface of ice and water, thereby inhibiting their growth (*2*). The inhibition occurs by preferential adsorption of the

---

F. D. Sonnichsen and B. D. Sykes, Protein Engineering Network of Centres of Excellence and Department of Biochemistry, University of Alberta, Edmonton, Alberta, T6G 2S2, Canada.
H. Chao and P. L. Davies, Department of Biochemistry, Queen's University, Kingston, Ontario, K7L 3N6, Canada.

*To whom correspondence should be addressed.